Journal Name

ARTICLE

Toxicity of 12 metal-based nanoparticles to algae, bacteria and protozoa

Villem Aruoja,*[a] Suman Pokhrel,[b] Mariliis Sihtmäe,[a] Monika Mortimer,[a] Lutz Mädler,[b] Anne Kahru[a]

The use of metal based nanoparticles (NPs) is increasing which leads to their release in water bodies *via* various waste streams and warrants risk assessment. Consistent biological effect data on NPs for environmentally relevant test species that are accompanied by thorough characterization of NPs are scarce but indispensable for understanding possible risks of NPs. We composed and tested a library of 12 metal-based nanoparticles (Al_2O_3, Co_3O_4, CuO, Fe_3O_4, MgO, Mn_3O_4, Sb_2O_3, SiO_2, ZnO, TiO_2, WO_3 and Pd) using alga *Pseudokirchneriella subcapitata*, three bacterial species (*Vibrio fischeri, Escherichia coli, Staphylococcus aureus*) and protozoan *Tetrahymena thermophila*. The NPs were characterized for physico-chemical properties, solubility and abiotic reactive oxygen species (ROS) production. Also, respective soluble salts were analysed for toxic effects. The algal growth inhibition assay proved the most sensitive and yielded EC_{50} values for 10 NPs ranging from 0.1 to 58 mg/l. Algal toxicity correlated with abiotic ROS production of NPs and the majority of NPs formed agglomerates that entrapped algal cells. Despite of different sensitivity, there was a common trend in the toxicity of NPs across different species and test formats: CuO and ZnO had highest toxicity (EC_{50} values below 1 mg/l) to all organism groups except protozoa. The high toxicity was mostly due to shedding of toxic concentrations of Zn and Cu ions; for most of the test species Al_2O_3, SiO_2, WO_3 and Sb_2O_3 were not toxic below 100 mg/l and MgO showed no adverse effect below 100 mg/l to any test species in any test setting.

Nano impact

The lack of good quality nanotoxicity data for environmentally relevant test species accompanied by physico-chemical characterization of nanoparticles (NPs) severely hampers risk assessment. This study provides biological response data of a thoroughly characterized library of metal-based NPs using algal, bacterial and protozoan tests. It includes correlations between NP properties and toxicity, as well as results obtained in deionized water, thus eliminating medium-specific effects. Similar trends across species are shown, although algae proved the most sensitive. EC_{50} values of 10 NPs ranged from 0.1 to 58 mg/l. The values may be used for toxicity modelling or directly for risk assessment, as the 72 h algal growth inhibition data are mandatory for the registration of chemicals in the European Union.

Introduction

Applications for metal-based nanoparticles (NP) are increasing rapidly, leading to concerns related to their effects in the environment.[1,2]

The novel properties of NPs that drive advances in technology could also determine possible environmental harm caused by these new substances. Despite the large number (>40000) of nano-toxicology studies there is still a lack of consistent toxicity data that could be used for risk assessment and modelling. The high variability of published toxicity values is related to the inherent complexity of the NPs: the substances with the same chemical formula can form particles with different properties leading to EC50 values that differ several

orders of magnitude.[3] Therefore, thorough physico-chemical characterisation of NPs should be included in such studies. The lack of good data is reflected in the limited number of computational models related to nano-toxicity, so far only a few examples of Quantitative Nano-structure Activity-Relationships (QNARs) based on bacterial toxicity data can be found in the literature,[4] while usable models of NP ecotoxicity are yet to be published.

This paper aims to provide a homogenous dataset of a metal-based NP library prepared and analyzed using the same methods. Altogether 12 NPs (Al_2O_3, Co_3O_4, CuO, Fe_3O_4, MgO, Mn_3O_4, Sb_2O_3, SiO_2, ZnO, TiO_2, WO_3 and metallic Pd) with primary sizes from 8 to 21 nm were synthesized and used for the analysis. The goal was to create a library of NPs that differ

in only one property – elemental composition. The NPs were chosen according to the needs of the European Union (EU) Seventh Framework Programme project MODERN (MODeling the EnviRonmental and human health effects of Nanomaterials; http://modern-fp7.biocenit.cat/) that focuses on development of a modelling framework for the environmental and health impacts of engineered NPs. The selection was based on the analysis of existing literature on metal oxide NP libraries[5-8] and intended to include both, toxic and non-toxic NPs, in order to analyse the physico-chemical properties that determine toxicity.

Four of the selected NPs (Al_2O_3, SiO_2, TiO_2, ZnO) belong to the list of 13 representative reference NMs selected by the OECD Working Party on Manufactured Nanomaterials to support measurement, toxicology and risk assessment of nanomaterials.[9]

In the current paper we address potential ecotoxicological hazard of metal-containing NPs, assessing their toxicity at three trophic levels, namely to the alga *Pseudokirchneriella subcapitata* as a primary producer protozoan *Tetrahymena thermophila* as a consumer and three bacterial species (*Vibrio fischeri, Escherichia coli, Staphylococcus aureus*) as decomposers. All these organism groups are relevant for aquatic toxicity testing. In addition, *Tetrahymena* as well as *Vibrio fischeri* data on organic chemicals have been used extensively for toxicity modelling.[10,11]

It is important to note that the algal growth inhibition assay is among the three tests (acute tests with crustaceans, algae and fish) mandatory in the framework of the EU chemical safety policy, REACH (Registration, Evaluation, Authorisation and Restriction of Chemicals)[12] according to which all chemicals manufactured or imported in the amount of 1 tonne/year or more in the European market have to be characterized for their potential impact on aquatic ecosystems by 2018. Considering the lack of algal toxicity data for NPs (Figure S1), our results are likely to be useful for regulatory purposes.

Materials and methods

Synthesis of nanoparticles

For the synthesis of NPs analysed in a current study a flame spray pyrolysis (FSP) was used. This technique allows obtaining crystalline particles with similar size and large specific surface area. An FSP reactor and the process of NP synthesis have been described previously.[13-15] Briefly, the metal-organic precursors (zinc napthenate, copper napthenate, cobalt napthenate, iron napthenate, manganese napthenate, titanium (IV) isopropoxide, antimony (III) isopropoxide, aluminium secondary butoxide, tetraorthosilicate (TEOS), magnesium napthenate, hexacarbonyl tungsten and palladium acetylacetonate) were dissolved in highly combustible organic solvent such as xylene to dilute the precursor and bring the metal concentration to 0.5 M. All chemicals were 99.9 % pure, purchased from Sigma-Aldrich. Each liquid precursor was delivered to the nozzle tip by a syringe pump at a flow rate of 5 ml/min by atomising the precursor solution with dispersant O_2 at a flow rate of 5 ml/min and maintaining a pressure drop of 1.5 bar at the nozzle tip. Combustion of the dispersed droplets was initiated by the co-delivery of CH_4 and O_2 (1.5 and 3.2 l/min respectively) to form a flame. The particles are formed at temperatures ~3000 K in the flame environment during combustion of the dispersed droplets. Eventually, the NP aerosol is quenched to room temperature with cold gas and the NPs are collected with a filter unit.

X -ray diffraction studies

X -ray diffraction was used for structural analysis of the synthesized NPs**.** For the X-ray diffraction measurements, the NPs were loaded in a D8 or PANalytical X'Pert MPD PRO diffracting unit, equipped with Ni-filtered Cu-K_α (λ=0.154 nm) radiation. The structural and microstructural parameters were extracted using Rietveld refinement by applying BRASS program. Background, scale factor, unit cell parameters, Gaussian as well as Lorentzian peak widths parameters were simultaneously refined followed by crystallite size and microstrain analysis. For all the materials, the crystal structures were refined to yield accurate positions of the atoms. The determination of the average crystallite sizes (d_{XRD}) was achieved by the line-broadening analysis. The instrumental contribution to the peak broadening was removed by the deconvolution method with crystalline LaB_6 as an instrumental standard.

Brunauer-Emmett-Teller (BET) analysis of nanoparticles

The BET method was used to determine the specific surface area (SSA) of the samples. The SSA values were used for calculation of primary particle sizes. N_2 adsorption-desorption measurements were carried out at 77 K using a Quantachrome NOVA 4000e Autosorb gas sorption system. The NPs were placed in a test cell and allowed to degas for 2 hours at 200 °C in flowing nitrogen. Data were obtained by introducing or removing a known quantity of adsorbing gas in or out of a sample cell containing the solid adsorbent maintained at a constant liquid nitrogen temperature. The primary particle size was derived using the equation $d_{BET} = 6/(\rho_p \cdot S_A)$, where d_{BET}, ρ_p and S_A are defined as the average diameter of a spherical particle, theoretical density and the measured specific surface area, respectively.

TEM imaging

A small amount of the powders was dispersed in 5 ml of ethanol (AR grade, Strem) and sonicated in an ultrasonic bath for 60 minutes. A drop of the dispersed colloidal solution was placed on a copper grid. The samples were dried in ambient air and large areas of the sample were scanned before the investigation of the particle morphology. High and/or low resolution microscopic imaging of the specimens were investigated with a FEI Titan 80/300 microscope equipped with a Cs corrector for the objective lens, a Fischione high angle annular dark field detector (HAADF), a Gatan post-column imaging filter and a cold field emission gun operated at 300 kV as an acceleration voltage. Imaging was performed at several time points in order to identify the homogeneity of the samples. Selected area diffraction pattern (SAED) analyses were performed as described in Pokhrel et al., 2010.[16]

Preparation and characterization of nanoparticle suspensions

About 5 mg of each nanopowder was weighed and mixed with about 25 ml of deionized (DI) water (Milli-Q, Millipore, USA) to yield 200 mg/l stock suspensions that were vortexed and sonicated for 4 minutes before use (40 W, Branson probe sonicator, USA). Hydrodynamic size and ζ-potential of the 100 mg/l NP suspensions in both DI water as well as algal medium[17] (Table 1) were measured using Malvern Zetasizer Nano-ZS (Malvern Instruments, Malvern, UK). Toxicity tests were conducted in three different media: DI water (bacterial 'spot' assay and protozoan assay), algal test medium (*P. subcapitata* growth inhibition test) and 2 % NaCl (*Vibrio*

Table 1 Physico-chemical properties of nanoparticles and their suspensions in the test media (deionized water and algal growth medium). Soluble metals were measured after incubation under conditions of the algal growth inhibition assay as described in Materials and methods.

Sample	Specific surface area (SSA); m2/g	BET size (d_{BET}) nm	DI water					Algal growth medium (pH=8.0)			
			z-average hydrodynamic size, nm	ζ-potential, mV	pH	Metal solubility		z-average hydrodynamic size, nm	ζ-potential, mV	Metal solubility	
						% at 10 mg/l (AAS or ICP-MS*)	% at 200 mg/l (TXRF)			% at 10 mg/l (AAS or ICP-MS*)	% at 100 mg/l (TXRF)
ZnO	53	20.4	171	16.4	6.6	56.1*	5.0	696	-13.1	25.7	3.18
Pd	33	15.1	127	-27.8	6.1	<0.5	NA	151	-18.6	0.24	NA
CuO	72	13.1	130	17	6.2	5.14	0.88	769	-6.2	1.16	0.26
Co_3O_4	85	11.5	99	23	6.1	1.25	6.8	916	10.7	0.18	0.82
TiO_2	123	12.2	171	-13.6	6.2	<0.83	0.10	717	-15.1	0.42	0.01
Mn_3O_4	81	15.2	395	-14.4	7.0	11.1	4.8	920	-9.8	9.45	6.62
Fe_3O_4	120	9.7	128	22.2	5.9	<1.38	7.1	1005	-12.1	1.66	0.17
Al_2O_3	134	11.4	95	39.2	6.0	0.40*	NA	1232	8.9	0.42	NA
SiO_2	289	7.8	148	-33.2	6.0	NA	NA	154	-19.8	NA	NA
WO_3	79	10.6	63	-45.3	5.0	63.2*	2.3	191	-20.4	66.7	75.7
MgO	123	13.6	1964	6.9	9.6	38.1	NA	1581	6.4	87.9[†]	NA
Sb_2O_3	56	20.5	125	-24.3	4.2	56.3	NA	414	-15.9	21.2	NA

AAS – Atomic Absorption Spectroscopy, * - ICP-MS - Inductively Coupled Plasma Mass Spectrometry ,TXRF - Total Reflection X-Ray Fluorescence, NA – not analysed, [†] - includes Mg^{2+} present in the algal medium

fischeri luminescence inhibition assay). For toxicity experiments the NP stock suspensions were diluted with 200 % respective test medium in the ratio of 1:1 to obtain 100 mg/l suspensions in each medium.

Analysis of nanoparticle solubility in deionized water and algal medium

To mimic the dissolution of NPs in toxicity testing environment, NP suspensions in algal medium as well as in DI water were prepared as described above and incubated in the same conditions as for algal toxicity testing (the test with the longest incubation time). After 72 hours 4 ml of each suspension was pipetted into a centrifuge tube (7/16X2-3/8, Beckman Coulter Polyallomer Centrifuge Tubes) and centrifuged using Beckman ultracentrifuge L8-M at 390,000 g for 40 minutes. After centrifugation, 3 ml of the supernatant was carefully removed, acidified with ultrapure HNO_3 (puriss, Sigma-Aldrich), heated for 3 h at 80 ℃ and analysed for respective metals either by using graphite furnace atomic absorption spectroscopy (GF-AAS, Varian SpectrAA 220, detection limit ~ 10 ppb; analysis was performed by a certified laboratory at Tallinn University of Technology (TUT), Department of Chemistry, Laboratory of Chemical Analysis), or, in the case of Zn, Al and W, using ICP-MS (X-Series 2, Thermo Scientific, detection limit 0.1 ppb; analysis was performed by Institute of Geology, TUT). It was not possible to analyse Si with the available equipment. In parallel, the concentration of metals in the supernatants as well as in NP suspensions was quantified using total reflection X-ray fluorescence spectroscopy (TRXF) Picofox S2 (Bruker AXS Microanalysis GmbH, detection limit 1 ppb). For this, NP suspension was mixed with gallium (Ga) internal standard in the ratio of 1:1 and 5 µl of this mixture was pipetted onto a quartz carrier disc. Concentration of metals was quantified with Spectra software (AXS Microanalysis GmbH).

Analysis of stability of nanoparticle suspensions in deionised water and algal medium

NP suspensions were prepared as described above, sonicated, diluted in the ratio of 1:1 with either DI water or 200 % algal medium and analysed immediately in a 1 cm path quartz cuvette using either UV-Vis spectrophotometry (Multiskan Spectrum, Thermo Electron Corp., Finland) or dynamic light scattering (count rate) (Malvern Zetasizer Nano-ZS, Malvern Instruments, UK).

Analysis of nanoparticles-induced abiotic reactive oxygen species in abiotic conditions

Two different fluorescent probes were used to estimate formation of reactive oxygen species (ROS) by the NPs: 2′,7′-dichlorodihydrofluorescein (H_2DCF), which reacts with a wide range of reactive oxygen and nitrogen species and the hydroxyl radical (OH·) specific 3'-(p-hydroxyphenyl) fluorescein (HPF, Life Technologies). In order to simulate conditions of the algal assay, the incubation was carried out in the same temperature and light conditions but also in the dark. The incubation lasted up to 72 hours with HPF, however, because H_2DCF decomposes under illumination the results using this probe were recorded within 45 minutes.

2,7-dichlorodihydrofluorescein diacetate assay. The fluorescent dye 2′,7′-dichlorodihydrofluorescein diacetate (H_2DCF-DA, Life Technologies) is a reagent often used to assess total ROS generation by nanoparticles.[18] Briefly, 1 ml of H_2DCF-DA (dissolved in ethanol at 1.3 mM) was freshly deacetylated to H_2DCF by reacting with 4 ml of 0.01 N NaOH for 30 min in the dark. The reaction was stopped by adding 20 ml of 25 mM sodium phosphate buffer (pH 7.4) to form a 52 µM H_2DCF solution. The mixture was immediately placed on ice and protected from light until use. After that, 100 µl of NP suspension and 100 µl of H_2DCF solution were pipetted to each well of a 96-well black microplate and the mixture was

incubated at room temperature for 45 minutes. At the end of incubation, fluorescence (excitation at 485 nm and emission at 527 nm) was quantitated using microplate fluorometer (Fluoroskan Ascent FL, Thermo Labsystems, Helsinki, Finland). As a positive control to induce the oxidation of H_2DCF to a fluorescent 2',7'-dichlorofluorescein (DCF), Fenton reaction was used. In this case, a similar procedure as the one described in case of NPs was used but the mixture of H_2O_2 (1.27 mM) and $FeSO_4x7H_2O$ (1 mM) dilutions were used instead of NPs suspensions. Abiotic ROS level was calculated as follows:

$$F = \frac{F_{t45(sample)}}{F_{t45(control)}}$$

where

$F_{t45(sample)}$ is the fluorescence of NP solution in DI water (t=45 min) after incubation with the fluorescent dye;

$F_{t45(control)}$ is the fluorescence of blank DI water (t=45 min) after incubation with the fluorescent dye. Fluorescence is presented in relative fluorescence units (RFU).

   3'-(p-hydroxyphenyl) fluorescein assay. HPF was used to measure the hydroxyl radical generation by nanoparticles as essentially described in.[19] Briefly, 100 µl of NP suspensions (200 mg/l) in DI water and 100 µl of HPF solution (10 µM) in 25 mM sodium phosphate buffer (pH 7.4) were pipetted into the wells of a 96-well black microplate and incubated for 72 h. Experiments were carried out both in the dark at room temperature and under illumination, using the same light and temperature conditions as in algal toxicity assay. For incubation under lamps the microplates were covered with glass plate, in order to ensure similar conditions to the algal test that was performed in glass vials. Fluorescence (excitation at 485 nm and emission at 527 nm) was quantitated using a fluorescence plate reader (Fluoroskan Ascent FL). Abiotic ROS induction was calculated as described above in the case of H_2DCF-DA assay.

Vibrio fischeri kinetic bioluminescence inhibition assay (a Flash-test)

Acute bioluminescence inhibition assay (exposure time 30 minutes) with bacteria *Vibrio fischeri* was performed at room temperature (~20 °C) in 96-well microplates following the Flash-assay protocol.[20,21] To 100 µl of test suspension in the microplate well 100 µl of bacterial suspension was added by automatic dispensing in the luminometer testing chamber. The luminescence was recorded during the first 10 s after dispensing of the bacteria in each well without additional mixing of the sample. After 30 min incubation the luminescence was recorded again (Figure S2). The Microplate Luminometer Orion II (Berthold Detection Systems, Pforzheim, Germany), controlled by Simplicity Version 4.2 Software was used. Reconstituted *V. fischeri* Reagent (Aboatox, Turku, Finland) was used as the test bacteria suspension and all chemicals and their dilutions were prepared in 2 % NaCl. Each test was performed in 5–7 replicates. Controls, both negative (2 % NaCl) and positive (3,5-dichlorophenol, 3,5-DCP), were included in each measurement series. The inhibition of bacterial luminescence (INH%) by the analysed compounds was calculated as follows:

$$INH\% = 100 - \frac{IT_{30}}{KF * IT_0} * 100 \quad \text{with} \quad KF = \frac{IC_{30}}{IC_0};$$

KF (correction factor) characterizes the natural loss of luminescence of the control (i.e. bacterial suspension in 2 % NaCl). IC_0 and IT_0 are the maximum values of luminescence during first 5 seconds after dispensing of 100 µl of test bacteria to 100 µl of control or test sample, respectively. IC_{30} and IT_{30} are the respective luminescence values after 30 minutes. EC_{50} is the concentration of a compound reducing the bioluminescence by 50 %.

Bacterial and algal viability assay ('spot test')

The 'spot test' described in detail by Kasemets *et al.* (2013)[22] and Suppi *et al.* (2015)[23] was used to test the ability of the toxicant-exposed bacteria and algae to form colonies on toxicant-free nutrient agar after 24 h exposure to the tested chemicals in deionised water (bacteria) or algal test medium (algae). Both, gram-positive (*Staphylococcus aureus* RN4220) and gram-negative (*Escherichia coli* MG1655) bacteria with different structure of the cell envelope as well as the alga *P. subcapitata* were used. Briefly, 100 µl of the bacterial or algal suspension was added to 100 µl of varying concentrations of NPs in either DI water, or, in the case of alga, also in the algal medium.

   Dilution series of 1:10 (1:3 for the alga) of the NP suspensions in the range of 0.01-100 mg/l (nominal concentrations) were tested.

   Bacteria and algae were exposed to NPs in 96-well microplates (non-tissue culture treated, BD Falcon) at 25 °C for 24 h without shaking in the dark, or, in the case of alga, under illumination comparable to the algal growth inhibition test. After 24 h of exposure to the toxicants (or DI water/medium), 5 µl of the cell suspension from each microplate well was pipetted as a 'spot' onto agarised LB growth medium (bacteria) or agarised algal growth medium (algae). The inoculated agar plates were incubated for 24 h at 30 °C. For the algal 'spot test' the inoculated Petri dishes with agarised algal growth medium (Table S1) were incubated at ~25 °C in constant light for several days until growth of algae was visible. Minimal biocidal concentration (MBC) of the tested NPs/chemicals was determined as the lowest tested nominal concentration of a chemical which completely inhibited the ability of the cells to form visible colonies after plating onto toxicant-free agar-plates. 3,5-DCP was used as a positive control. Each experiment was repeated two or three times.

Cell viability assay with protozoa *Tetrahymena thermophila*

Protozoan culture (*T. thermophila* strain BIII) was cultivated essentially as described by Mortimer et al. 2010. The cells were harvested during the exponential growth phase (5×10^5 cells/ml) by centrifugation at 500 g for 5 min at 4 °C and washed twice with DI water. The cell density was determined by counting in a haemocytometer (Neubauer Improved, bright line; Germany) after immobilisation in 5 % formalin.

   For toxicity analysis 100 µl of harvested and washed *T. thermophila* suspension in DI water was added to 100 µl of the solution/suspension of NPs or the respective water-soluble salts that were previously diluted in DI water in 96-well polystyrene plates. Each concentration was tested in at least three replicates and the final cell density in the test was 5×10^5 cells/ml.

   Protozoan suspension and metal compounds in DI water were used as non-treated and abiotic controls, respectively. The

test plates were incubated in 25 °C in the dark. After 24 h exposure 50 µl of the cell suspension was sampled from each well, and viability of the cells was determined by measuring the ATP content essentially as previously described.[24] Briefly, ATP was extracted from the protozoan cells with 0.5 % trichloroacetic acid (TCA) and 2 mM ethylenediamine-tetraacetic acid (EDTA) and the samples were stored at -18 °C until analysis. Prior to analysis the samples were thawed and diluted 5-fold with Tris–EDTA buffer (0.1 mM Tris, 2 mM EDTA, adjusted to pH 7.75 with acetic acid). 100 µl of the diluted samples were transferred to the wells of a white 96-well microplate and, after measuring the background light emission, mixed with equal volume of ATP Assay Mix (FL-AAB, Sigma-Aldrich) which was previously diluted 500-fold with ATP Assay Mix Dilution Buffer (FL-AAM, Sigma-Aldrich). 10 µl of ATP standard (10^{-5} M) was used for internal calibration. All the luminescence measurements were done using Orion II plate luminometer (Berthold Detection Systems, Germany). The amount of the ATP in each well was calculated according to the following equation:

$$ATP, \mu mol = \frac{RLU_{sample} - RLU_{background}}{RLU_{ATPstandard}} \times ATP\,standard$$

The ATP concentrations in the samples were expressed as percentages of the non-treated controls. The EC_{50} values (effective concentration leading to a 50 % cell death) was calculated from the concentration-effect curves as described below.

Algal growth inhibition assay with *Pseudokirchneriella subcapitata*

The assay procedure adhered to OECD guideline 201 for algal growth inhibition assay[17] and is described in detail in Aruoja et al., (2009)[25]. Briefly, the *P. subcapitata* stock culture for inoculation was obtained from the commercial test system Algal Toxkit F (MicroBioTests Inc., Nazareth, Belgium). The number of the algal cells in the inoculum was determined by counting under light microscope in the Neubauer haemocytometer. Exponentially growing algal cultures were exposed to various concentrations of NP suspensions/metal salts and incubated at 24 ± 1 °C for up to 72 h in standard 20 ml glass scintillation vials containing 5 ml of algal growth medium (OECD, 2011; Table S1). The vials were illuminated from below with Philips TL-D 38 W aquarelle fluorescent tubes (see SI for details). All samples were run in duplicate with four controls distributed evenly on the transparent plate. A dilution series of $ZnSO_4$ was included in all experiments as a positive control. Algal biomass was measured at least every 24 hours by quantifying the fluorescence of algal pigment extract. The fluorometric method has been found to be the most suitable for nanoparticle assays.[26] For that 50 µl of culture samples were transferred to a 96-well black polypropylene plate (Greiner Bio-One), 200 µl of ethanol was added to each sample and the plate was shaken for 3 h in the dark. Thereafter the fluorescence was measured with a microplate fluorometer (excitation 440 nm, emission 670 nm; Fluoroscan Ascent, Thermo Labsystems, Finland). EC_{50} values (effective concentration leading to 50 % reduction of biomass) were calculated from dose-response data as described below.

The cell concentration of the control culture increased at least 16 times during 3 days. The variability between replicates was kept low by using the vials only once. The coefficient of variation of biomass density in replicate control cultures throughout the experiments did not exceed 5 %.

Analysis of nutrient adsorption to nanoparticles

In order to assess the potential growth inhibition of algae due to adsorption of algal medium components (nutrients) onto studied NPs as well as inhibition caused by particle dissolution, algal growth inhibition test was carried out with ultra-centrifuged supernatants of NP suspensions. For that the NP suspensions that showed toxicity to *P. subcapitata* below the 100 mg/l level were prepared, diluted to concentrations that were expected to be inhibitory based on the assay with suspensions, incubated on a shaking plate under the same conditions as algal growth inhibition test for 3 days and subsequently centrifuged as described above.. The carefully removed supernatants were used for algal toxicity testing.

Calculation of EC_{50} values

The toxicity values (EC_{50}) for the algal growth inhibition, *V. fischeri* luminescence inhibition and *T. thermophila* viability assays and their confidence intervals were determined from dose–response curves by the REGTOX software for Microsoft Excel[27] using the Log-normal model. All NP concentrations used for EC_{50} calculations were nominal.

Results and discussion

Characterization of nanoparticles

The synthesised Al_2O_3, Co_3O_4, CuO, Fe_3O_4, MgO, Mn_3O_4, Sb_2O_3, SiO_2, ZnO, TiO_2, WO_3, and metallic Pd NPs were highly crystalline according to low-resolution transmission electron microscopy (TEM) and selected area diffraction patterns (SAED) (Figure S3). The specific surface area and primary particle size of these materials were in the range of 33 to 289 m^2/g and 8-21 nm, respectively (*Table* 1), which reasonably agree with the size, determined using XRD (Table S2). For a subset of eight NPs, the primary particle sizes were also confirmed by TEM analysis (Figure S3, Table S2). The TEM micrographs demonstrate the particle shapes as well as their tendency to aggregate under dry conditions. The weight percentage of anatase and rutile in TiO_2 was 12.4 and 87.6 % respectively, that is typical for FSP synthesized TiO_2 nanoparticles (Figure S4). Fe_3O_4 had a two phase mixture of hematite (Fe_2O_3) and magnetite (Fe_3O_4) with 64.7 % and 35.3 % by weight (Figure S5).

Characterization of nanoparticle suspensions

The ζ-potential of the particle suspensions and the hydrodynamic size of the particles varied considerably depending on the medium (*Table* 1). pH values of the initial NP suspensions were not adjusted. In general, pH values of NP suspensions in DI water at 100 mg/l were in the range of 5.9–6.9. However, WO_3 and Sb_2O_3 were acidic and MgO was alkaline (*Table* 1). The pH of NP suspensions in the algal medium was 8 ± 0.5. While most of the studied particles formed relatively stable suspensions in DI water, all NPs, except SiO_2 and WO_3, agglomerated and settled quickly when suspended in the algal medium (Figures S6, S7). There was linear correlation between hydrodynamic size (z-average) of NP suspensions and absolute ζ-potential in the algal medium, whereas in DI water all NPs had a comparable hydrodynamic size (<200 nm), except MgO and Mn_3O_4 that formed larger agglomerates (Figure S8). Sedimentation of particles was also

mostly dependent on ζ-potential, although water suspensions were more stable at absolute ζ-potential values <20 mV compared to suspensions in the algal medium (Figure S9). Interestingly, most of the WO_3 appeared to dissolve when suspended in the algal medium, according to both UV-Visible spectroscopy (Figure S7) as well as chemical analysis data (Table 1), while being much less soluble in DI water. WO_3 has also been found to dissolve (20-25 %) in Dulbecco's Modified Eagle's Medium (DMEM), even though the analysis was carried out after centrifugation of NPs at much lower speed (20,000 g) than in the current study.[28]

Toxicity of nanoparticles

The library of NPs was analysed using three different bacterial species, protozoan and alga. Bacterial and algal cells should *a priori* be resistant to NP entry due to their rigid cell wall, whereas protozoa are naturally particle-ingesting and tend to sequester NPs in the food vacuoles that may lead to different mechanisms of toxicity.[24] Bacteria and unicellular alga are thus useful in studying the toxicity arising from the solubilized fraction of metallic NPs. Both, gram-positive (*Staphylococcus aureus*) and gram-negative (*E. coli*, *V. fischeri*) bacterial species were used in order to compare bacteria with different structure of the cell envelope. Algae were represented by *P. subcapitata*, a freshwater species known to be sensitive to metals, including metal-containing NPs.[3,25,29] In addition, the OECD algal growth inhibition test is an important assay for REACH and can be used to study NPs with only minor modifications. Previous studies using this assay have shown particle agglomeration/cell entrapment as well as nutrient adsorption onto NPs.[25,30] Therefore, the latter two aspects were studied in more detail in the current study. The mechanisms of algal toxicity were assessed more closely than in case of other test species because of higher sensitivity of the algal growth inhibition assay towards metal-based NPs.[3] The upper concentration limit of 100 mg/l was chosen based on the hazard ranking criteria for aquatic environment, which states that substances with an $L(E)C_{50}$ >100 mg/l are not considered harmful (i.e., they are "not classified").[31]

Toxicity to bacteria

Higher toxicity of NPs compared to the respective bulk formulations (if applicable) to microorganisms has been attributed to their nano-size that causes cell-membrane damage and generation of ROS.[32] In the case of certain metal containing NPs (e.g. Ag, CuO and ZnO) solubilized metal ions have been shown to contribute to their toxicity to bacterial cells.[3,4,33] Comparison of the toxic effects of silver NPs with different sizes showed that smaller NPs were more toxic due to higher dissolution rate.[29]

Bacterial viability assay ('spot test') with *Escherichia coli* and *Staphylococcus aureus*. The microbial 'spot-test' is a novel approach that uses DI water as the test environment for NP toxicity evaluation.[23] Exposure in DI water minimizes the effect of speciation that strongly influences the bioavailability and toxicity of metal containing NPs in organic-rich but also in mineral test media. This assay format thus allows comparing the 'effective' toxic concentrations of NPs to different organisms by eliminating the variation introduced by test media with variable metal-complexing potential. On the other hand, due to the lack of buffer in the test medium there may be pH-related effects on toxicity values. Results from the 24 h 'spot' assay with bacteria showed that the most toxic in this test

format was CuO (24 h MBC to *S. aureus* was 0.1 mg/l and to *E. coli* 1 mg/l), followed by ZnO (MBC to both bacteria 10 mg/l) and Pd (MBC for *S. aureus* was 100 mg/l and for *E. coli* 10 mg/l). Co_3O_4, Fe_3O_4 and Mn_3O_4 were of medium toxicity showing growth inhibitory effects at 100 mg/l level at least to one bacterial strain. Al_2O_3, MgO, Sb_2O_3, SiO_2 and TiO_2 and WO_3 were not toxic to *E. coli* and *S. aureus* below 100 mg/l in this test format (Figure 1, Table **2**). Thus, the absence of buffer did not appear to influence the MBC values as neither the sample with the lowest nor the highest pH (Sb_2O_3, pH=4.2 and MgO, pH=9.6, respectively) inhibited bacterial growth. However, in the case of Sb_2O_3 some reduction in growth was evident (Figure 1). Concerning cell envelope type (gram positive or negative bacteria) there was no clear relationship observed. In the case of CuO and Mn_3O_4 gram-positive bacteria (*S. aureus*) were slightly more susceptible (MBC 0.1 and 100 mg/l, respectively) than gram-negative bacteria (*E. coli*) (MBC 1 and >100 mg/l). The higher susceptibility of gram-positive bacteria to metal-based biocidal chemicals (including Cu^{2+} and Zn^+) has been previously reported and explained by differences in bacterial cell envelope structures, e.g., some heavy metal transport proteins are poorly represented in gram-positive bacteria due their lack of the outer cellular membrane.[34,35] We have also previously shown that *S. aureus* was more susceptible to silver than *E. coli*.[23] However, analogous sensitivity pattern was not observed for Co_3O_4 and Pd (Figure 1, Table **2**) as gram-negative *E. coli* (MBC 100 and
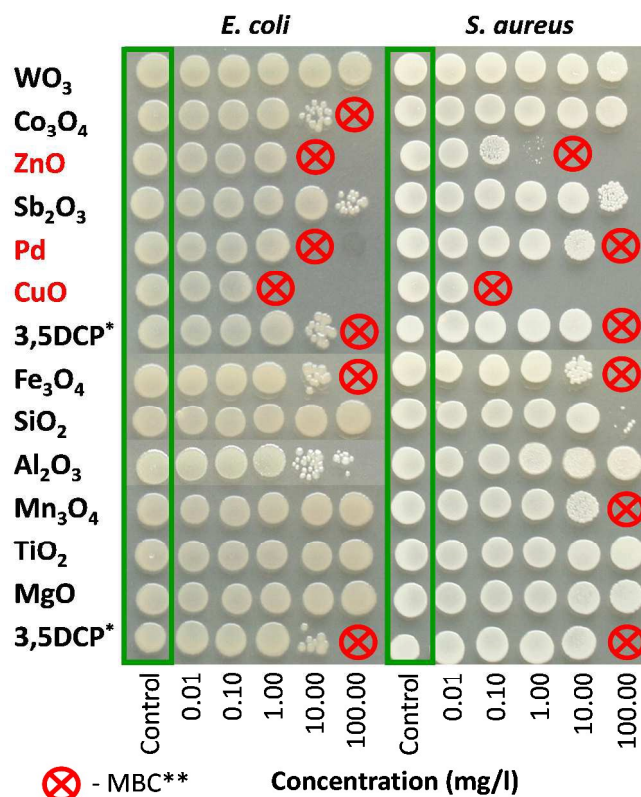

Figure 1. Toxicity of 12 nanoparticles to bacteria *Escherichia coli* and *Staphylococcus aureus*. Toxicity was evaluated by colony-forming ability of the bacteria after exposure to nanoparticles in deionised water for 24 h at 25 °C. After exposure, 5 μl of bacterial suspension was transferred onto toxicant-free agarized LB growth medium. The concentrations of the NPs are in mg compound/l. All concentrations are nominal. * - 3,5 dichlorophenol was used as a positive control. ** - Minimal biocidal concentration.

10 mg/l, respectively) was more sensitive than gram-positive *S. aureus* (MBC >100 and 100 mg/l). The results are comparable to the data obtained by other authors for metal-based NPs. Among the 12 tested NPs in the current study the greatest antibacterial activity has been shown for CuO, ZnO (24 htoxicity values for both NPs ranged from 1 to 116 mg/l, depending on test and media used[23,36-38]) and Pd (24 h IC50 ≥1 mg/l[39]). Lower antibacterial activities have been demonstrated for Co_3O_4 (24 h MBC 128-256 mg/l, 24 h IC50 138 mg/l[38,40]), Al_2O_3 (24 h toxicity values >10 mg/l[41,42]), Sb_2O_3 (24h EC_{50} 266 mg/l[37]), Fe_3O_4/Fe_2O_3 (24 h toxicity values >65 mg/l[36,43]) and SiO_2 (24 h IC50 ~20 mg/l[41]) NPs.

Kinetic bioluminescence inhibition assay (flash-test) with *Vibrio fischeri.* The kinetic *V. fischeri* luminescence inhibition assay (flash assay) is an ISO standardized acute toxicity test.[20] It is a very rapid, simple, cost effective and sensitive method to evaluate/screen toxic properties of different chemical substances (including synthetic NPs[21] and solid/coloured environmental samples, e.g. sediments, soil suspensions, wastewater, sludge extracts, etc.[44,45]) by measuring the reduction of light production due to interactions between bacteria and toxic compounds. The decrease in bacterial luminescence occurs already after brief contact of bacteria with toxicants (in the scale of seconds to minutes, depending on the

compounds; Figure S2).[21] The decrease in bioluminescence reflects the inhibition of bacterial metabolic activity and is proportional to the toxicity of test sample.[46] Considering that NP suspensions are often turbid due to agglomeration of particles, the kinetic format of the *V. fischeri* test is appropriate for the toxicity screening of NPs.[21] The flash assay data were in general agreement with the 'spot test': the most toxic NPs were CuO, ZnO and Pd with the 30-min EC_{50} values of 1.8, 11.5 and 55 mg/l, respectively (Table S3, Figure 2, Table **2**). Also Sb_2O_3 and WO_3 showed toxic effects at <100 mg/l level that could be attributed to suboptimal pH in the test environment (pH around 5, see Table 1).

The rest of the NPs (Al_2O_3, Co_3O_4, Fe_3O_4, Mn_3O_4, MgO, SiO_2, TiO_2,) had EC_{50} values >100 mg/l. It should be mentioned that pH values higher than optimal to bacteria (9.6 in the case of MgO) did not appear to inhibit the luminescence of *V. fischeri*. These data are in general agreement with previously reported toxicity values (15 or 30 minute EC_{50}, mg/l) for *V. fischeri*: ZnO 1.9-7.8;[21,33,47,48] CuO 7.8-204;[21,33,47,49] MgO 61.9;[47] Fe_3O_4 240;[50] SiO_2 381.[48] No toxicity of TiO_2 NPs to *V. fisheri* has been shown in dark exposure conditions.[33,51] In addition to the NPs the respective soluble metal salts were tested using the *V. fischeri* bioluminescence inhibition assay (Table S3). The high toxicity of copper and zinc ions (EC_{50} 0.42 and 2.7 mg metal/l, respectively)
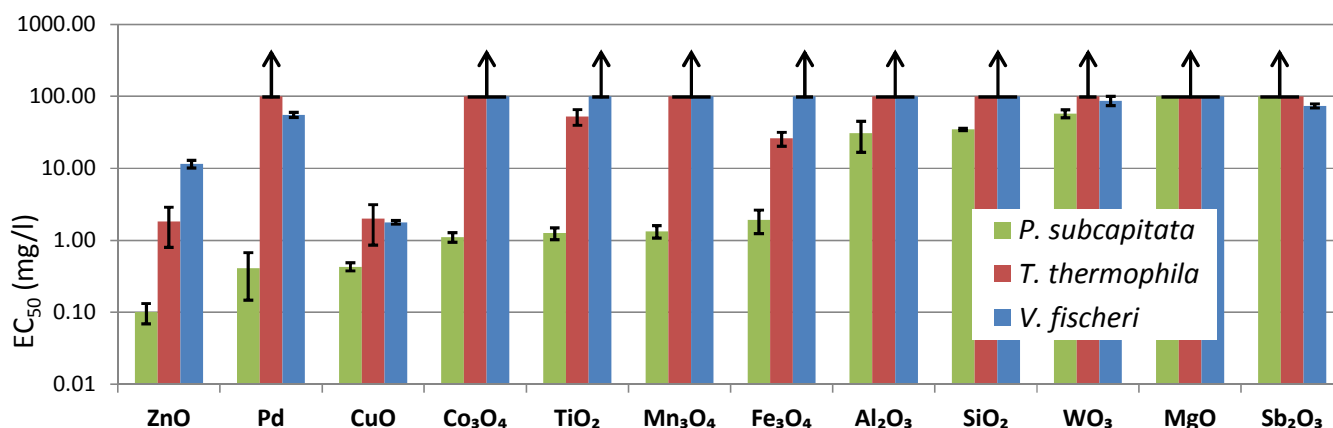

Figure 2. Toxicity of 12 nanoparticles to alga *Pseudokirchneriella subcapitata*, protozoan *Tetrahymena thermophila* and bacterium *Vibrio fischeri*. EC_{50} values were obtained from 72 h algal growth inhibition assay, 24 h *T. thermophila* viability assay and 30-min *V. fischeri* luminescence inhibition assay (Table S3). Arrows indicate EC_{50} values above 100 mg/l. Concentrations are nominal.

indicates that the toxic effects of CuO and ZnO towards *V. fischeri* were probably mediated by shed metal ions (see Table 1). The same mechanism seems to be true for Sb and Pd ions (2.03 and 0.23 mg metal/l, respectively) but in this case we observed also suboptimal pH of the test environment (see Table S3) as 2 % NaCl has no buffering capacity. However, the acidic pH had insignificant effect on bacterial viability in the 'spot test' (24 h MBC values for both WO_3 and Sb_2O_3 were >100 mg/l) (Figure 1).

Toxicity to protozoa *Tetrahymena termophila*

In protozoan assays the 24 h EC_{50} values of NPs could be calculated for only 4 particles that showed toxicity <100 mg/l (ZnO – 1.8, CuO – 2.0, Fe_3O_4 – 26 and TiO_2 – 53), as shown in Table S3, Figure 2 and Table **2**. The protozoan assay, analogously to algal and bacterial tests, showed that CuO and ZnO NPs were the most toxic, acting already at 1-2 mg/l level.

Fe_3O_4 was also toxic to algae and bacteria *E. coli* and *S. aureus* and TiO_2 was toxic to algae (Figure 2; Table **2**). The toxicity of ZnO to *T. thermophila* is coherent with data obtained by Mortimer *et al.* (2008)[24] (24 h EC_{50} 6 mg/l) but the CuO used in the current study was more toxic than the CuO purchased from Sigma studied by us previously[24] (EC_{50}=160 mg/l), probably due to different solubilization rates. Also differently from our studies 15 nm TiO_2 (anatase) NPs were not acutely toxic to *T. thermophila* (24 h EC_{50}>1000 mg/l).[52]

Protozoa are highly relevant test organisms for nanotoxicology as they are ecologically widely spread particle-feeding organisms.[53] Protozoa are also important in wastewater treatment.[54] The first nanotoxicological studies on protozoa concerned carbon nanomaterials[55,56] followed by metal-containing NPs such as CuO and ZnO,[24,57,58] TiO_2[52] and QDs.[59-61]

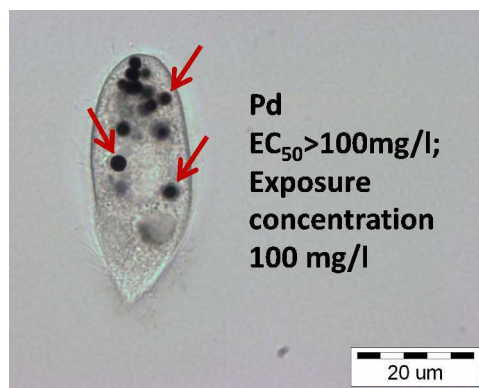The first papers published on effects of NPs on feeding

Figure 3. Bright field microscopy image of *Tetrahymena thermophila* after incubation with Pd NPs for 24 h. Dark Pd agglomerates in the food vacuoles are clearly visible.

behaviour of *T. thermophila* showed that they ingested single walled carbon nanotubes (SWNTs) and bacteria as food with no apparent discrimination, however, SWNTs inhibited bacterivory of protozoa starting from 3.6 mg SWNT/l level whereas the effects on viability were observed starting from 6.8 mg SWNT/l. The authors concluded that the inhibiting effect of SWNTs on protozoan bacterivory could have negative impact on normal ecological processes.[62] Moreover, accumulation of NPs in protozoa may exert harmful effects via food-web transfer of NMs.[59] Also, Mortimer *et al*. (2014)[60] who studied uptake and trafficking of subtoxic amounts of CdSe/ZnS QDs on *T. thermophila* concluded that long residence times of NPs in protozoa increase the risks of transfer of these NPs to higher trophic levels in the ecosystem.

Therefore, although most of the NPs in the current study showed no toxic effects on protozoa at exposure levels below 100 mg/l (Table S3; Figure 2), they may still exert harmful effects to the ecosystem via trophic transfer of NPs. This is illustrated on Figure 3 that shows extensive accumulation of Pd NPs in food vacuoles of *T. thermophila* after 24 h exposure to the subtoxic concentration of Pd NPs.

Toxicity to alga *Pseudokirchneriella subcapitata*

Experimentally determined EC_{50} values based on *P. subcapitata* growth inhibition are listed in Table S3 and plotted on Figure 2. 72 h EC_{50} values ranged from 0.10 mg/l for ZnO and 0.43 mg/l for CuO till 57.8 mg/l (WO₃), spanning three orders of magnitude. Only MgO and Sb₂O₃ were not toxic to algae (EC_{50} >100 mg/l). The *P. subcapitata* toxicity values (Table S3) are generally in agreement with previously published scarce algal toxicity data (see also Figure S1). The reported median EC_{50} values collected from the literature are for ZnO 0.08 mg/l, for CuO 2.8 mg/l[3] and for TiO₂ 65.5 mg/l[62]. SiO₂ NPs (a commercial LUDOX silica preparation) 72 h EC_{20} values for 12.5 and 27.0 nm sized particles were 20 and 28.8 mg/l, respectively. EC_{50} values were not reported in the study.[63] Metzler *et al*. (2012)[64] reported that TiO₂ (42 nm in diameter) had EC_{20} of 5.2 mg/l, Al₂O₃ (14–18 nm) 5.1 mg/l and SiO₂ 318 mg/l. Al₂O₃ 72 h EC_{50} values of growth inhibition have been reported for *Chlorella sp*. (45.4 mg/l) and *Scenedesmus sp*. (39.4 mg/l).[65]

Figure 2 shows that algae were by far the most sensitive test organisms when compared to bacteria and protozoa. Analogously, in their review on ecotoxicity of synthetic NPs (including ZnO, CuO and TiO₂) Kahru and Dubrouguier

(2010)[62] showed that algae and crustaceans were the most sensitive and thus probably the 'weakest link' in aquatic exposure to NPs. For the above reasons, the algal toxicity was studied in more detail, as described below.

NP toxicity to alga: proposed mechanisms

There is a number of mechanisms proposed for the toxic action of metal/metal oxide NPs, including: toxicity of soluble metal that leaches from the particles; ROS generation by NPs with or without light energy; ROS generation by the soluble metal; co-agglomeration of NPs and cells that physically isolates cells from nutrients/light energy; sequestration of medium components by NPs.[4,30] The observed toxicity responses are likely the result of a combination of these and other mechanisms, some of which are discussed below.

Solubility. Our previous study demonstrated that the algal toxicity of ZnO and CuO NPs (purchased from Sigma-Aldrich) was solely explained by bioavailable metal ions leaching from the particles.[25] The same has been shown for other test organisms such as bacteria, yeasts and crustaceans.[3,29,33,66] The toxicities of NPs, the respective soluble salts and theoretical solubility of NPs at their EC_{50} concentrations are plotted on Figure 4. The soluble fractions are calculated based on metal concentrations measured in 10 mg/l NP suspensions incubated in the conditions of the algal growth inhibition assay (Table 1) and may thus be inaccurate as the fraction depends on the NP concentration (overestimated in the case of EC_{50} values >10 mg/l and underestimated for values <10 mg/l).
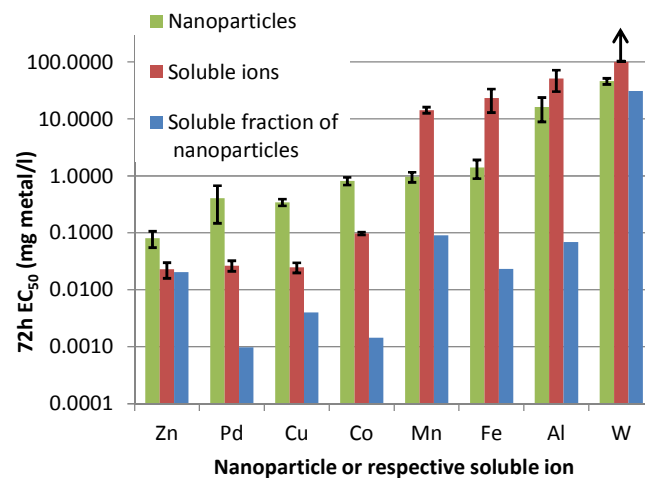

Figure 4. Solubilisation explains toxic effect of ZnO, but not other nanoparticles (NPs) to alga: 72 h EC_{50} values (nominal concentrations on a metal basis, mg/l) of NPs (green) and respective soluble salts (red; Table S3). Blue bars denote theoretical amount of dissolved metals in NP dispersions at the 72 h EC_{50} concentrations (calculated based on solubility data in Table **1**). Note the logarithmic scale of Y-axis. Arrow indicates EC_{50} value above 100 mg/l.

Nevertheless, according to this comparison only ZnO toxicity can be fully explained by the soluble fraction of zinc. Despite previous reports of CuO NP toxicity due to soluble copper the CuO in the current study appeared less prone to solubilisation in the mineral algal medium. Examination of the dose-response curves of metal salts on algal growth (not shown) revealed no toxicity at the calculated soluble metal concentrations in the case of other NP on Figure 2, except for tungsten (W) that showed some toxicity near the EC_{10} value. Based on the EC_{50}

values of NPs and soluble salts NPs formed two distinctive groups: 1) NPs, which were less toxic compared to the respective soluble salts (ZnO, Pd, CuO, Co_3O_4), and 2) NPs which had higher toxicity than their soluble salts (Mn_3O_4, Fe_3O_4, Al_2O_3, WO_3). The latter group warrants further research of the specific toxic effects of these materials.

Agglomeration/entrapment. We have previously studied the effects of ZnO, CuO and TiO_2 NPs to alga *P. subcapitata* and witnessed entrapment of algal cells in TiO_2 NP suspensions.[25] In the current study the formation of agglomerates that contained algal cells and NPs was observed for most of the studied NPs, only excluding ZnO, WO_3, SiO_2 and Sb_2O_3 (Figure 5, Figure S10). There was no apparent correlation between the average hydrodynamic size or ζ-potential of the NPs in suspension and their potency to entrap algae.

Toxic concentration of ZnO was very low (EC_{50} 0.1 mg/l) and it is therefore likely that all the particles were dissolved at this level. WO_3 was one of the least toxic substances; however, it also dissolved almost fully in the algal medium. WO_3 suspension in DI water was the only truly "nano" suspension, with particle hydrodynamic size below 100 nm (63 nm; Table 1). Moreover, the WO_3 in the algal medium never had any visible sediment and so it is likely that the WO_3 particles that remained insoluble were well dispersed, despite the change in ζ-potential (-45 mV in DI water vs -20 mV in algal medium; Table 1). We were unable to determine the solubility of SiO_2, but according to literature amorphous silica has a solubility of 2.0 mmol/l (120 mg/l) at around pH 7 and 25 °C[67]. Considering that silica NPs may dissolve beyond the equilibrium concentration value,[65,68] it is possible that SiO_2 was fully dissolved in our experiments. On the other hand, based on light scattering (count rate) data (Figure S6) SiO_2 formed a stable suspension (hydrodynamic size of particles 154 nm) in the algal medium (Table 1).Sb_2O_3 was partly dissolved (21 %; Table 1) at 10 mg/l level, so there should have been sufficient amount of particles at 100 mg/l level for agglomeration and subsequent entrapment of algae to occur. Also, the ζ-potential of Sb_2O_3 in the algal medium was only slightly more negative than TiO_2 (-15.85 *versus* -15.05 mV) which formed typical agglomerates. Nevertheless, no clumping or toxicity of Sb_2O_3 was observed.

The clumps in the cultures with Al_2O_3 and MgO were loose formations of algal cells whereas in the suspensions that proved more toxic, i.e. more growth inhibitory to algae such as Pd, CuO, Co_3O_4, TiO_2, Mn_3O_4, Fe_3O_4 the agglomerates entrapped nearly all algal cells so that the cells could mostly be seen inside the agglomerates using fluorescence microscopy and only rarely in the surrounding medium (Figure S10).

Similar agglomeration/entrapment has been documented previously for Al_2O_3 NPs in the case of other algal species such as *Scenedesmus* sp. and *Chlorella* sp.[65] Analogous entrapment has been shown for carbon nanotubes (CNT) with *Chlorella vulgaris*.[69] In this case the photosynthetic activity of the entrapped algae was not affected and the growth inhibition was explained by reduced availability of light and locally elevated algal concentration inside the CNT agglomerates. In the current study, the viability of algal cells exposed to NPs in DI water was estimated using the 'spot' assay (see Materials and methods) and was found to be remarkably higher than could be expected based on the algal growth inhibition test (Figure S11). For example, the EC_{50} of Pd in the growth inhibition test was 0.4 mg/l, and the minimal biocidal value (24 h MBC) in DI water based on the 'spot' assay was 10 mg/l. In addition, when

a single agglomerate of Pd containing algal cells was transferred to a clean medium, algal growth resumed (data not shown), indicating viability of entrapped cells.
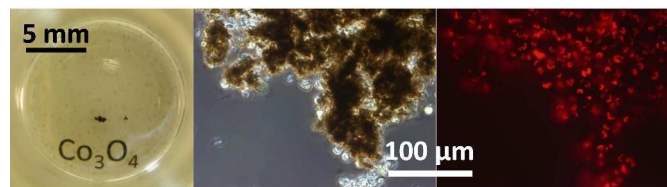

Figure 5. Nanoparticle agglomerates entrap algae. Examples of NP agglomerates that entrapped algal cells visible with a naked eye (A), in phase contrast microscope (B) and fluorescence microscope (C); other examples are shown in Figure S10.

The large agglomerates occurred only in the presence of the algal cells, *i.e.* there were no visible clumps in abiotic controls (Figure S10). The ζ-potential of the algal cells was negative (-25.4 mV) similarly to most of the nanoparticles, excluding electrostatic interaction as a driving force for agglomerate formation. Various algal species are known to increase the production of exopolymeric substances (EPS) in response to NP exposure, which may be a general algal defence mechanism against (metal containing) toxicants. For example, *Chlamydomonas reinhardtii* cells formed "tightly packed flocks" with EPS in the presence of CeO_2 NPs[70] while silver NP toxicity to the marine diatom *Thalassiosira weissflogii* was reduced in nutrient limited cells that produced more EPS, suggesting the role of EPS in Ag^+ detoxification.[71] Similar results were obtained with diatom algae exposed to copper and cadmium ions: production of extracellular polysaccharides was increased in response to the toxicants which in turn increased metal tolerance of the algae.[72] Thus, while the EPS may protect algal cells against toxic metals, the agglomeration caused by the same substances during the algal growth inhibition assay appeared to decrease the obtained EC_{50} values. Nevertheless, algal growth inhibition assay has proven far more sensitive than the 'spot' assay also for "conventional" soluble chemicals that do not entrap algae, such as $AgNO_3$: the 24 h MBC (in DI water) was 10 mg $AgNO_3$/l[23] whereas the 72 h EC_{50} in the growth inhibition assay was 0.007 mg Ag/l.[29]

Abiotic reactive oxygen species (ROS) generation by NPs in abiotic conditions. One of the main paradigms of NP toxicity is considered to be ROS generation that results in oxidative stress.[53,73] In the current study we used two fluorescent probes to estimate radical formation by the NPs: 3'-(p-hydroxyphenyl) florescein (HPF) that is specific to the hydroxyl radical ($OH\cdot$)[74] as well as 2′,7′-dichlorodihydrofluorescein (H_2DCF), that reacts with a wide range of ROS.[75] In both cases the assays were conducted in the abiotic conditions, i.e. without test organisms, under the same light and temperature conditions as the algal growth inhibition test as well as in the dark.

Both HPF and H_2DCF assay identified the same NPs as the most potent in generating ROS (Figure 6, A, C). TiO_2 was by far the most effective in generating $OH\cdot$ radicals, but only under illumination, no radical production was detected in the dark (Figure 6, B, D). It is widely known that TiO_2 NPs produce $OH\cdot$ under UV or near UV-light (at wavelengths below 388 nm),[76] but are generally not photo-reactive under visible light. In fact, different approaches such as doping with Pt or Fe have been used to increase TiO_2 photo-reactivity under visible light.[19,77] Apparently, the fluorescent tubes used for
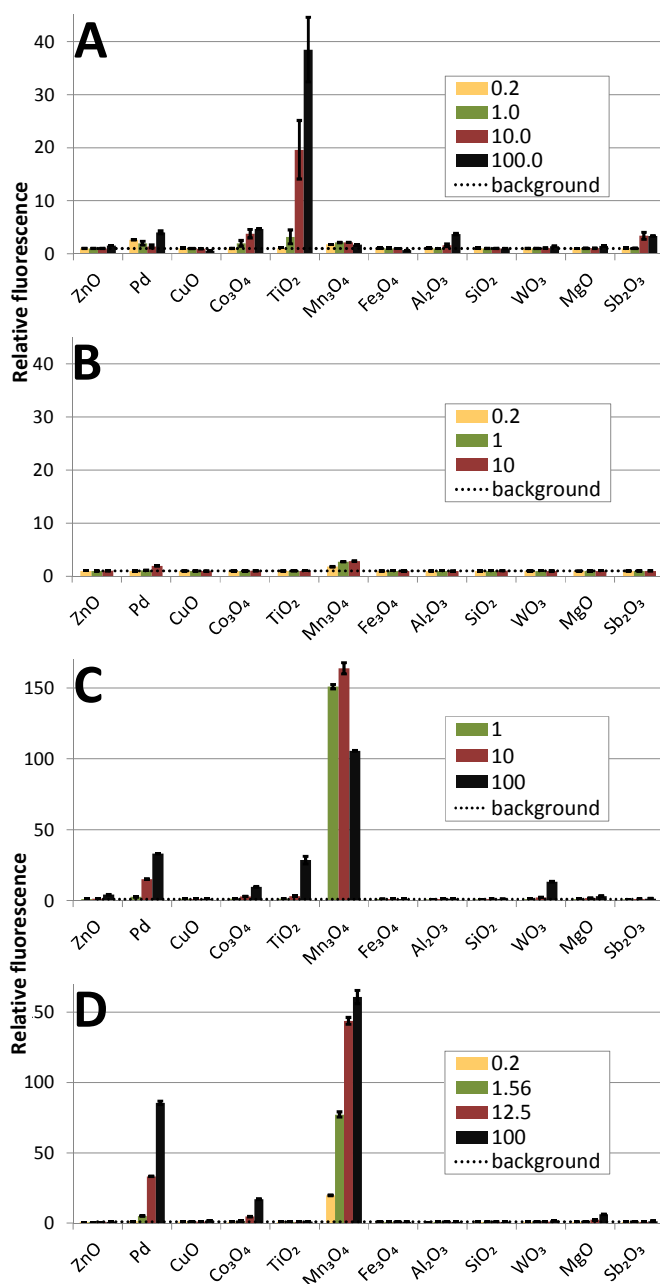
Figure 6. Abiotic generation of reactive oxygen species (ROS) by studied nanoparticles under illumination (A, C) and in the dark (B, D), measured with florescent dyes HPF (A, B) and H2DCF (C, D). For HPF the highest values during 3-day incubation are plotted, whereas the values after 45 minute incubation are shown for H2DCF (H2DCF loses its fluorescence in a few hours when exposed to light and could not be incubated for the entire duration of the algal test). Concentrations are shown in the insets and are nominal, in mg/l. Dotted line indicates background = 1.0.

illumination during algal culturing provided sufficient light energy (see SI for the specification of the fluorescent tubes) to excite electrons and induce OH· generation of FSP-synthesized TiO2 with band gap energy of 3.1 eV (equivalent to 400 nm). An order of magnitude smaller fluorescence signal (indicative of ROS) was recorded for Co3O4, Pd, Al2O3 and Sb2O3 (Figure 6). In the H2DCF assay the strongest signal was generated by Mn3O4, followed by Pd and Co3O4. These three
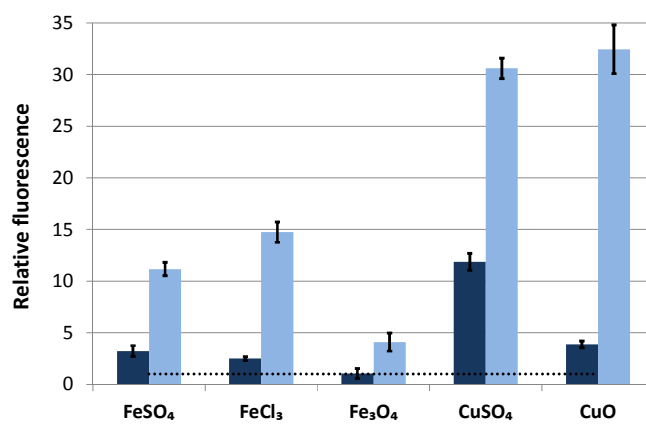

Figure 7. Abiotic generation of reactive oxygen species (ROS) by iron and copper ions and respective NPs in the presence of H2O2 during 24 h in the dark (dark bars) and under illumination (light bars); NP nominal concentration is 10 mg/l, corresponding to 0.13 mM (Fe) and 0.12 mM (Cu) based on metal atoms; concentration of all three soluble salts is 0.13 mM. Dotted line indicates background = 1.0.

NPs generated ROS without photo-activation, although Co3O4 and Pd may generate some additional OH· radicals under illumination, according to the HPF assay. ROS appeared to contribute to the toxicity of TiO2, Mn3O4, Co3O4 and Pd NPs that were identified as potent ROS generators by both fluorescent assays while their EC50 values in growth inhibition assay of *P. subcapitata* were all below 1.5 mg/l. However, the causal link between ROS production and toxicity remains unclear. The algal cell wall should prevent NP entry into cells and only extracellularly produced ROS can contribute to the observed toxic effects. Indeed, NP-derived ROS may damage algal cell membrane from outside, as indicated by oxidative stress related increase in membrane permeability of *P. subcapitata*, due to CeO2 NPs.[30] On the other hand, there are some reports of NP internalization into algal cells, concerning CuO particles: 5 nm particles of CuO into the prokaryotic alga *Microcystis aeruginosa*[78] and CuO as well as polymer-coated CuO particles with a primary size of 30-40 nm into *C. reinhardtii*.[79] In the latter report, 6.5 times higher amounts of polymer-coated NPs compared to bare CuO were found inside cells. Still, The ZnO, CuO and Fe3O4 NPs reported here were highly toxic to the alga, but did not appear to produce ROS, unlike similar particles in other investigations.[80] It has been shown that iron oxide NPs release

soluble iron that generates hydroxyl radicals *via* the Fenton reaction[81] and the surface of Fe3O4 NPs has been found to be a potent catalyst of OH· radical formation in the presence of H2O2.[82] Since Cu ions are also known to catalyse Fenton-like reactions[83] we tested Fe3O4 and CuO NPs additionally in the presence of H2O2. The result, shown on **Figure 7**, indicates that the Fe3O4 and CuO NPs used in our study were much less potent compared to respective ions when tested in the dark; however, under illumination CuO was the most active Fenton catalyst.

Adsorption of nutrients onto nanoparticles. It has been shown that CeO2 NPs deplete phosphate as well as micronutrients Fe and Mo from the algal growth medium[30] that may cause growth inhibition. In order to verify this possibility the NP suspensions were incubated with the algal growth medium, ultra-centrifuged and the supernatants used for

toxicity testing. This approach does not distinguish nutrient depletion from toxicity arising from the solubilized fraction of NPs and is therefore difficult to interpret in the case of readily soluble NPs. Based on solubility data (Table 1); however, it is likely that the toxicity of ZnO supernatant is due to dissolved zinc (Figure S12). For CuO, TiO_2, Fe_3O_4, Co_3O_4, Mn_3O_4 and Pd there was no toxicity at concentrations several times higher than the EC_{50} of the respective NP suspensions, excluding any influence of nutrient depletion. SiO_2 and Al_2O_3 supernatants (of 92.7 mg/l suspensions) showed some toxicity which may have had a small influence on the corresponding EC_{50} values, however, in the case of SiO_2 the effect may have been due to solubility. Interestingly, the supernatant of WO_3 suspension (92.7 mg/l) showed complete inhibition of algal growth, in agreement with high solubility ($\approx$70 %) of WO_3 in the algal

medium (Table 1) but in disagreement with the (lower) toxicity of the soluble Na_2WO_4.

Comparison of the toxicity of 12 nanoparticles across species and test formats

In order to compare the toxic effects of studied 12 NPs to different test species we grouped test-wise the NPs according to their EC_{50} values (Table **2**). This classification adheres to EU-Directive 93/67/EEC (CEC 1996) and is based on the lowest median $L(E)C_{50}$ value of the three key environmental organisms: algae, crustaceans and fish; <1 mg/l = very toxic to aquatic organisms; 1–10 mg/l = toxic to aquatic organisms; 10–100 mg/l = harmful to aquatic organisms; >100 mg/l = not classified.

Table 2 Categorization of NPs based on the toxicity values (EC_{50} or MBC, mg compound/l) to bacteria, protozoa and algae. All NPs were tested in nominal concentrations from 0.01 up to 100 mg/l. Data are summarised from Table S3

EC_{50} or MBC, mg compound/l	72 h EC_{50}	24 h EC_{50}	30 min EC_{50}	24 h MBC	24 h MBC
Organisms:	Algae	Protozoa	Bacteria	Bacteria	Bacteria
Species:	*Pseudokirchneriella subcapitata*	*Tetrahymena thermophila*	*Vibrio fischeri* (*G-*)	*Escherichia coli* (*G-*)	*Staphylococcus aureus* (*G+*)
Exposure medium:	Mineral medium	DI water	2 % NaCl	DI water	DI water
0.1-1	CuO, ZnO, Pd	None	None	CuO	CuO
>1-10	Co_3O_4, Fe_3O_4, Mn_3O_4, TiO_2	CuO, ZnO	CuO	ZnO, Pd	ZnO
>10-100	Al_2O_3, SiO_2, WO_3	Fe_3O_4, TiO_2	ZnO, Pd, WO_3, Sb_2O_3	Co_3O_4, Fe_3O_4	Fe_3O_4, Mn_3O_4, Pd
>100	MgO, Sb_2O_3	Al_2O_3, Co_3O_4, MgO, Mn_3O_4, Pd, Sb_2O_3, SiO_2, WO_3	Al_2O_3, Co_3O_4, Fe_3O_4, MgO, Mn_3O_4, SiO_2, TiO_2	Al_2O_3, MgO, Mn_3O_4, Sb_2O_3, SiO_2, TiO_2, WO_3	Al_2O_3, Co_3O_4, MgO, Sb_2O_3, SiO_2, TiO_2, WO_3

EC_{50} - half effective concentration; MBC – Minimal Biocidal Concentration, i.e., the lowest tested nominal concentration of NPs which completely inhibited the formation of visible colonies after sub-culturing on toxicant-free agarised growth medium. Prior subculturing bacteria were incubated with NPs for 24 h at 25 °C in deionised water.

The toxicity tests were carried out with unicellular organisms of different biological complexity: prokaryotic (bacteria) and eukaryotic (algae, protozoa). In terms of food web level algae are primary producers, protozoa consumers and bacteria decomposers. Also, the exposure times for the assays varied from 30 minutes (*V. fischeri* bioluminescence inhibition assay) to 72 h (algal growth inhibition test). In addition, protozoa are naturally particle-feeding organisms but bacteria and algae should be resistant to particles. Thus, theoretically only the soluble fraction of NPs and/or ROS produced outside of the cells could affect the viability of bacteria and algae. Table **2** shows that although the test species and test formats were different, there were common features in terms of toxic effects. CuO and ZnO were the most toxic NPs to all the test species regardless of the assay and toxicity endpoint. Also Pd was toxic to alga and bacteria *E. coli* at relatively low concentration (<10 mg/l) and Co_3O_4 showed toxic effects to alga (<10 mg/l) and *E. coli* (<100 mg/l). Although we did not include the data of the algal 'spot' test in Table 2 (Figure S9) it

pointed to the same direction: CuO, ZnO, Co_3O_4 and Pd were the most toxic in this assay format.

Table **2** shows that MgO was the only NP that was not toxic to any test organism in any test setting (i.e. EC_{50} or MBC > 100 mg/l), in addition to MgO, for the majority of test species and test settings Al_2O_3, Co_3O_4, Fe_3O_4, Mn_3O_4, SiO_2, TiO_2 showed no toxic effects below 100 mg/l. The most sensitive test was algal growth inhibition assay according to which only MgO and Sb_2O_3 proved not toxic even at 100 mg/l and CuO, ZnO and Pd showed growth inhibitory effects at very low concentrations (< 1 mg/l).

Conclusions and outlook

In this paper we analysed the toxicity of 12 metal-based NPs to the representatives of three important groups of aquatic species: algae, bacteria and protozoa. The particles were synthesized using the flame spray pyrolysis method, resulting in a library of crystalline NPs with similar primary size that were thoroughly characterized both as dry powders and suspensions in the

respective test media. As a result, a homogenous dataset of toxicity values and respective physic-chemical properties was created. The test suite involved species from different trophic levels whereas algae proved to be the most sensitive: within the set of NPs the algal toxicity values spanned 3 orders of magnitude that could be useful for further analysis and QNAR modelling.

Among the test species used in the current study, alga *P. subcapitata* was the most sensitive, as stated above, with EC_{50} values <100 mg/l for 10 out of 12 NPs tested, whereas in case of the protozoan *T. thermophila* EC_{50} values could be calculated only for four NPs and in case of the bacterium *V. fischeri* for five NPs.. However, although most of the studied NPs did not affect viability of protozoa below 100 mg/l, the remarkable accumulation of NPs in protozoan food vacuoles is a prerequisite for food-web transfer and bioaccumulation, thus a sign of potential harm.

The algal toxicity mechanisms were studied in more detail, revealing solubilisation as a probable cause of ZnO toxicity, whereas formation of ROS in abiotic conditions correlated with the toxicity of other NPs in the library.

Despite the similar primary particle size, the NPs with different elemental composition will form suspensions that have various levels of agglomeration/solubility, thus creating additional complexity. The cells in the toxicity assays will be subjected to agglomerates of NPs of different sizes and surface charges as well as varying concentrations of soluble ions leaching from the NPs, complicating the interpretations of the test results.

In order to understand the mechanisms of aquatic toxicity of NPs and ultimately move closer to toxicity prediction a quantitative approach to mechanisms is required. This approach should be usable across different organisms or even for the whole aquatic ecosystem and should therefore include data from a battery of test species belonging to different trophic levels, including, as a minimum, primary producers (e.g. algae), consumers (e.g. protozoa) and decomposers (bacteria). Whether the QNAR models based on one species (for example *P. subcapitata*, *T. thermophila*, *V. fischeri* or *E. coli*) could predict the toxic effects also to other aquatic organisms, remains to be elucidated. However, there is a good chance the answer is 'yes' as the results presented in this paper show remarkably similar toxic effects of metal-based NPs across species at different trophic levels and in a range of biotests.

Acknowledgements

Notes and references

[a] Laboratory of Environmental Toxicology, National Institute of Chemical Physics and. Biophysics, Akadeemia tee 23, Tallinn 12618, Estonia.

[b] Foundation Institute of Materials Science IWT, University of Bremen, Bremen, Germany.

1. A. Kahru and A. Ivask, *Accounts of Chemical Research*, 2013, 46, 823-833.
2. K. L. Garner and A. A. Keller, *J. Nanopart. Res.*, 2014, 16.
3. O. Bondarenko, K. Juganson, A. Ivask, K. Kasemets, M. Mortimer and A. Kahru, *Archives of Toxicology*, 2013, 87, 1181-1200.
4. A. Ivask, K. Juganson, O. Bondarenko, M. Mortimer, V. Aruoja, K. Kasemets, I. Blinova, M. Heinlaan, V. Slaveykova and A. Kahru, *Nanotoxicology*, 2014, 8, 57-71.
5. X. Hu, S. Cook, P. Wang and H.-m. Hwang, *Sci. Total Environ.*, 2009, 407, 3070-3072.
6. T. Puzyn, B. Rasulev, A. Gajewicz, X. Hu, T. P. Dasari, A. Michalkova, H.-M. Hwang, A. Toropov, D. Leszczynska and J. Leszczynski, *Nature Nanotechnology*, 2011, 6, 175-178.
7. R. Rallo, B. France, R. Liu, S. Nair, S. George, R. Damoiseaux, F. Giralt, A. Nel, K. Bradley and Y. Cohen, *Environ. Sci. Technol.*, 2011, 45, 1695-1702.
8. H. Zhang, Z. Ji, T. Xia, H. Meng, C. Low-Kam, R. Liu, S. Pokhrel, S. Lin, X. Wang, Y.-P. Liao, M. Wang, L. Li, R. Rallo, R. Damoiseaux, D. Telesca, L. Maedler, Y. Cohen, J. I. Zink and A. E. Nel, *ACS Nano*, 2012, 6, 4349-4368.
9. OECD, Organisation for Economic Cooperation and Development, Paris, France, 2012.
10. M. T. D. Cronin and T. W. Schultz, *Sci. Total Environ.*, 1997, 204, 75-88.
11. T. I. Netzeva and T. W. Schultz, *Chemosphere*, 2005, 61, 1632-1643.
12. EC, European Commission, Brussels, Belgium, 2006.
13. W. Y. Teoh, R. Amal and L. Maedler, *Nanoscale*, 2010, 2, 1324-1347.
14. S. George, S. Pokhrel, T. Xia, B. Gilbert, Z. Ji, M. Schowalter, A. Rosenauer, R. Damoiseaux, K. A. Bradley, L. Maedler and A. E. Nel, *ACS Nano*, 2010, 4, 15-29.
15. J. A. Kemmler, S. Pokhrel, L. Maedler, U. Weimar and N. Barsan, *Nanotechnology*, 2013, 24.
16. S. Pokhrel, J. Birkenstock, M. Schowalter, A. Rosenauer and L. Madler, *Cryst. Growth Des.*, 2010, 10, 632-639.
17. OECD, Organisation for Economic Cooperation and Development, Paris, France., 2011.
18. E. K. Rushton, J. Jiang, S. S. Leonard, S. Eberly, V. Castranova, P. Biswas, A. Elder, X. Han, R. Gelein, J. Finkelstein and G. Oberdoerster, *Journal of Toxicology and Environmental Health-Part a-Current Issues*, 2010, 73, 445-461.
19. S. George, S. Pokhrel, Z. Ji, B. L. Henderson, T. Xia, L. Li, J. I. Zink, A. E. Nel and L. Maedler, *Journal of the American Chemical Society*, 2011, 133, 11270-11278.
20. ISO, International Organization for Standardization, Geneva, Switzerland, 2010.
21. M. Mortimer, K. Kasemets, M. Heinlaan, I. Kurvet and A. Kahru, *Toxicology in Vitro*, 2008, 22, 1412-1417.
22. K. Kasemets, S. Suppi, K. Kuennis-Beres and A. Kahru, *Chemical Research in Toxicology*, 2013, 26, 356-367.
23. S. Suppi, K. Kasemets, A. Ivask, K. Künnis-Beres, M. Sihtmäe, I. Kurvet, V. Aruoja and A. Kahru, *Journal of Hazardous Materials*, 2015, 286C, 75-84.
24. M. Mortimer, K. Kasemets and A. Kahru, *Toxicology*, 2010, 269, 182-189.
25. V. Aruoja, H. C. Dubourguier, K. Kasemets and A. Kahru, *Sci. Total Environ.*, 2009, 407, 1461-1468.
26. N. B. Hartmann, C. Engelbrekt, J. Zhang, J. Ulstrup, K. O. Kusk and A. Baun, *Nanotoxicology*, 2013, 7, 1082-1094.
27. E. Vindimian, 2009.
28. H. Y. Zhang, Z. X. Ji, T. Xia, H. Meng, C. Low-Kam, R. Liu, S. Pokhrel, S. J. Lin, X. Wang, Y. P. Liao, M. Y. Wang, L. J. Li, R. Rallo, R. Damoiseaux, D. Telesca, L. Madler, Y. Cohen, J. I. Zink and A. E. Nel, *ACS Nano*, 2012, 6, 4349-4368.

29. A. Ivask, I. Kurvet, K. Kasemets, I. Blinova, V. Aruoja, S. Suppi, H. Vija, A. Kaekinen, T. Titma, M. Heinlaan, M. Visnapuu, D. Koller, V. Kisand and A. Kahru, *PLoS One*, 2014, 9.

30. N. J. Rogers, N. M. Franklin, S. C. Apte, G. E. Batley, B. M. Angel, J. R. Lead and M. Baalousha, *Environ. Chem.*, 2010, 7, 50-60.

31. EC, Official J. of the European Union, European Commission, Brussels, Belgium, 2008.

32. J. H. Niazi and M. B. Gu, *Toxicity of metallic nanoparticles in microorganism – a review. Kim, Y. J.; Platt, U.; Gu, M.B.; Iwahashi , H. (Eds). In: Atmospheric and Biological Environmental Monitoring*, Springer, Netherlands, 2009.

33. M. Heinlaan, A. Ivask, I. Blinova, H.-C. Dubourguier and A. Kahru, *Chemosphere*, 2008, 71, 1308-1316.

34. J. P. Ruparelia, A. K. Chatteriee, S. P. Duttagupta and S. Mukherji, *Acta Biomaterialia*, 2008, 4, 707-716.

35. O. Bondarenko, T. Rolova, A. Kahru and A. Ivask, *Sensors*, 2008, 8, 6899-6923.

36. A. Azam, A. S. Ahmed, M. Oves, M. S. Khan, S. S. Habib and A. Memic, *International Journal of Nanomedicine*, 2012, 7, 6003-6009.

37. Y.-W. Baek and Y.-J. An, *Sci. Total Environ.*, 2011, 409, 1603-1608.

38. C. Kaweeteerawat, A. Ivask, R. Liu, H. Zhang, C. H. Chang, C. Low-Kam, H. Fischer, Z. Ji, S. Pokhrel, Y. Cohen, D. Telesca, J. Zink, L. Mädler, P. A. Holden, A. Nel and H. Godwin, *Environ. Sci. Technol.*, 2015, in press.

39. C. P. Adams, K. A. Walker, S. O. Obare and K. M. Docherty, *PLoS One*, 2014, 9.

40. T. Ghosh, S. K. Dash, P. Chakraborty, A. Guha, K. Kawaguchi, S. Roy, T. Chattopadhyay and D. Das, *Rsc Advances*, 2014, 4, 15022-15029.

41. W. Jiang, H. Mashayekhi and B. Xing, *Environmental Pollution*, 2009, 157, 1619-1625.

42. A. Simon-Deckers, S. Loo, M. Mayne-L'Hermite, N. Herlin-Boime, N. Menguy, C. Reynaud, B. Gouget and M. Carriere, *Environ. Sci. Technol.*, 2009, 43, 8423-8429.

43. M. Auffan, W. Achouak, J. Rose, M.-A. Roncato, C. Chaneac, D. T. Waite, A. Masion, J. C. Woicik, M. R. Wiesner and J.-Y. Bottero, *Environ. Sci. Technol.*, 2008, 42, 6730-6735.

44. J. Lappalainen, R. Juvonen, K. Vaajasaari and M. Karp, *Chemosphere*, 1999, 38, 1069-1083.

45. L. Pollumaa, A. Kahru, A. Eisentrager, R. Reiman, A. Maloveryan and A. Ratsep, *Atla-Alternatives to Laboratory Animals*, 2000, 28, 461-472.

46. A. A. Bulich, *Process Biochem.*, 1982, 17, 45-47.

47. T. Sovova, V. Koci, L. Kochankova and L. C. M. N. M. S. Tanger, *Ecotoxicity of nano and bulk forms of metal oxides*, 2009.

48. A. K. Safekordi, H. Attar and E. Binaeian, presented in part at the 2nd International Conference on Chemical, Ecology and Environmental Sciences (ICCEES'2012), Singapore April 28-29, 2012, 2012.

49. A. L. d. O. F. Rossetto, D. S. Vicentini, C. H. Costa, S. P. Melegari and W. G. Matias, *Chemosphere*, 2014, 108, 107-114.

50. A. Garcia, R. Espinosa, L. Delgado, E. Casals, E. Gonzalez, V. Puntes, C. Barata, X. Font and A. Sanchez, *Desalination*, 2011, 269, 136-141.

51. I. Lopes, R. Ribeiro, F. E. Antunes, T. A. P. Rocha-Santos, M. G. Rasteiro, A. M. V. M. Soares, F. Goncalves and R. Pereira, *Ecotoxicology*, 2012, 21, 637-648.

52. K. Rajapakse, D. Drobne, J. Valant, M. Vodovnik, A. Levart and R. Marinsek-Logar, *Journal of Hazardous Materials*, 2012, 221, 199-205.

53. A. Kahru, H. C. Dubourguier, I. Blinova, A. Ivask and K. Kasemets, *Sensors*, 2008, 8, 5153-5170.

54. G. Esteban, C. Tellez and L. M. Bautista, *Acta Protozoologica*, 1992, 31, 129-132.

55. Y. Zhu, T. Ran, Y. Li, J. Guo and W. Li, *Nanotechnology*, 2006, 17, 4668-4674.

56. Q.-F. Zhao, Y. Zhu, T.-C. Ran, J.-G. Li, Q.-N. Li and W.-X. Li, *Nuclear Science and Techniques*, 2006, 17, 280–284.

57. I. Blinova, A. Ivask, M. Heinlaan, M. Mortimer and A. Kahru, *Environmental Pollution*, 2010, 158, 41-47.

58. M. Mortimer, K. Kasemets, M. Vodovnik, R. Marinsek-Logar and A. Kahru, *Environ. Sci. Technol.*, 2011, 45, 6617-6624.

59. R. Werlin, J. H. Priester, R. E. Mielke, S. Kraemer, S. Jackson, P. K. Stoimenov, G. D. Stucky, G. N. Cherr, E. Orias and P. A. Holden, *Nature Nanotechnology*, 2011, 6, 65-71.

60. M. Mortimer, A. Kahru and V. I. Slaveykova, *Environmental Pollution*, 2014, 190, 58-64.

61. M. Mortimer, A. Gogos, N. Bartolome, A. Kahru, T. D. Bucheli and V. I. Slaveykova, *Environ. Sci. Technol.*, 2014, 48, 8760-8767.

62. A. Kahru and H. C. Dubourguier, *Toxicology*, 2010, 269, 105-119.

63. K. Van Hoecke, K. A. C. De Schamphelaere, P. Van der Meeren, S. Lucas and C. R. Janssen, *Environ. Toxicol. Chem.*, 2008, 27, 1948-1957.

64. D. M. Metzler, A. Erdem, Y. H. Tseng and C. P. Huang, *Journal of Nanotechnology*, 2012, 01/2012, 1-12.

65. I. M. Sadiq, S. Pakrashi, N. Chandrasekaran and A. Mukherjee, *J. Nanopart. Res.*, 2011, 13, 3287-3299.

66. K. Kasemets, A. Ivask, H.-C. Dubourguier and A. Kahru, *Toxicology in Vitro*, 2009, 23, 1116-1122.

67. J. Sonnefeld, A. Gobel and W. Vogelsberger, *Colloid Polym. Sci.*, 1995, 273, 926-931.

68. P. Born, F. C. Klaessig, T. D. Landry, B. Moudgil, J. Pauluhn, K. Thomas, R. Trottier and S. Wood, *Toxicological Sciences*, 2006, 90, 23-32.

69. F. Schwab, T. D. Bucheli, L. P. Lukhele, A. Magrez, B. Nowack, L. Sigg and K. Knauer, *Environ. Sci. Technol.*, 2011, 45, 6136-6144.

70. L. A. Rohder, T. Brandt, L. Sigg and R. Behra, *Aquatic Toxicology*, 2014, 152, 121-130.

71. A. J. Miao, K. A. Schwehr, C. Xu, S. J. Zhang, Z. P. Luo, A. Quigg and P. H. Santschi, *Environmental Pollution*, 2009, 157, 3034-3041.

72. R. Pistocchi, M. A. Mormile, F. Guerrini, G. Isani and L. Boni, *J. Appl. Phycol.*, 2000, 12, 469-477.

73. N. von Moos and V. I. Slaveykova, *Nanotoxicology*, 2014, 8, 605-630.

74. K. Setsukinai, Y. Urano, K. Kakinuma, H. J. Majima and T. Nagano, *J Biol Chem*, 2003, 278, 3170– 3175.

75. J. Y. Zhao and M. Riediker, *J. Nanopart. Res.*, 2014, 16, 13.

76. M. R. Hoffmann, S. T. Martin, W. Y. Choi and D. W. Bahnemann, *Chem. Rev.*, 1995, 95, 69-96.

77. M. J. Jing, Y. Wang, J. J. Qian, M. Zhang and J. J. Yang, *Chin. J. Catal.*, 2012, 33, 550-556.

78. Z. Y. Wang, J. Li, J. Zhao and B. S. Xing, *Environ. Sci. Technol.*, 2011, 45, 6032-6040.

79. F. Perreault, A. Oukarroum, S. P. Melegari, W. G. Matias and R. Popovic, *Chemosphere*, 2012, 87, 1388-1394.

80. Y. Li, W. Zhang, J. F. Niu and Y. S. Chen, *ACS Nano*, 2012, 6, 5164-5173.

81. A. S. Arbab, L. A. Bashaw, B. R. Miller, E. K. Jordan, B. K. Lewis, H. Kalish and J. A. Frank, *Radiology*, 2003, 229, 838-846.

82. M. A. Voinov, J. O. S. Pagan, E. Morrison, T. I. Smirnova and A. I. Smirnov, *Journal of the American Chemical Society*, 2011, 133, 35-41.

83. B. C. Gilbert, G. Harrington, G. Scrivens and S. Silvester, *EPR studies of Fenton-type reactions in copper-peroxide systems*, Kluwer Academic Publ, Dordrecht, 1997.

Environmental Science: Nano Accepted Manuscript